

Article

Influence of Hydrothermal Carbonization on Catalytic Fast Pyrolysis of Agricultural Biomass

Lukasz Niedzwiecki ^{1,2,*}, Krzysztof Moscicki ¹, Anton Bijl ^{3,4}, Pawel Owczarek ⁵, Amit Arora ⁶, Mateusz Wnukowski ¹, Christian Aragon-Briceno ⁷, Vishwajeet ¹, Halina Pawlak-Kruczek ¹, Eddy Bramer ³, Gerrit Brem ³ and Artur Pozarlik ³

¹ Department of Energy Conversion Engineering, Wrocław University of Science and Technology, Wyb. Wyspiańskiego 27, 50-370 Wrocław, Poland

² Energy Research Centre, Centre for Energy and Environmental Technologies, VŠB—Technical University of Ostrava, 17. Listopadu 2172/15, 708 00 Ostrava, Czech Republic

³ Department of Thermal and Fluid Engineering, University of Twente, Drienerlolaan 5, 7522 NB Enschede, The Netherlands

⁴ Alucha Works BV Westervoortsedijk 73, 6827AV Arnhem, The Netherlands

⁵ Feinor sp. z o.o., Poprężniki 19, 98-215 Goszczanów, Poland

⁶ Department of Chemical Engineering, Shaheed Bhagat Singh State University, Ferozepur 152004, Punjab, India

⁷ Fundacion Circe, Parque Empresarial Dinamiza, Avda. Ranillas 3D, 1ª Planta, 50018 Zaragoza, Spain

* Correspondence: lukasz.niedzwiecki@pwr.edu.pl

Featured Application: Optimum parameters of valorization of biomass for fast pyrolysis process.

Abstract: Fast pyrolysis has been a subject of intensive research thanks to its ability to produce high yields of liquid products, known as pyrolysis oil. This is an important renewable intermediate which could be used for the subsequent production of fuels and chemicals. For fossil-based materials, pyrolysis oil can provide circular building blocks. Furthermore, direct use of pyrolysis oil in gas turbines has also been proven feasible. However, a relatively high oxygen content in raw biomass has detrimental effects on the quality of such oil. This work proposes hydrothermal carbonization as a valorization technique, beneficial from the point of view of subsequent fast pyrolysis. Within the scope of this work, the influence of the parameters of hydrothermal carbonization (HTC) on the kinetics of fast pyrolysis of agricultural biomass (miscanthus), as well as the influence of in situ use of a CaO catalyst, is investigated. Kinetics is investigated using a novel type of thermogravimetric analyzer (TGA) called Cyclonic TGA, which is able to achieve heating rates similar to a real fast pyrolysis process. Moreover, the influence of HTC on the removal of part of its inorganic constituents is determined within the scope of this work.

Keywords: HTC; fast pyrolysis; miscanthus



Citation: Niedzwiecki, L.; Moscicki, K.; Bijl, A.; Owczarek, P.; Arora, A.; Wnukowski, M.; Aragon-Briceno, C.; Vishwajeet; Pawlak-Kruczek, H.; Bramer, E.; et al. Influence of Hydrothermal Carbonization on Catalytic Fast Pyrolysis of Agricultural Biomass. *Appl. Sci.* **2023**, *13*, 4190. <https://doi.org/10.3390/app13074190>

Academic Editor: María Ángeles Martín-Lara

Received: 28 February 2023

Revised: 20 March 2023

Accepted: 24 March 2023

Published: 25 March 2023



Copyright: © 2023 by the authors. Licensee MDPI, Basel, Switzerland. This article is an open access article distributed under the terms and conditions of the Creative Commons Attribution (CC BY) license (<https://creativecommons.org/licenses/by/4.0/>).

1. Introduction

Extensive effort is ongoing to fulfil the challenging climate goals which have been set by the agreement signed in Paris. Biomass is an upcoming renewable energy source, which has fulfilled around 19% of heating demand, as well as 3% of electricity demand in 2019 in the EU [1]. Due to these reasons, valorization of biomass has been intensively investigated recently, considering its tremendous potential [2–4].

Pyrolysis is a thermal process in which decomposition takes place in the absence of oxygen [5,6], thus converting biomass to a mixture of solid, liquid, and gaseous compounds [7–10] (unlike gasification, where partial oxidation takes place [11–13]). Solid products can be used as solid fuel or applied to soil in the form of biochar [14]. Gaseous products can be used on-site to supply the process heat. Condensable products can also be used on-site for energy needs. However, it is also possible to condense those compounds

and obtain pyrolysis oil, which can be considered an excellent energy carrier due to its relatively high energy density. A wide range of different processes comes under the common name of pyrolysis. Torrefaction is also known as mild pyrolysis [15–17]. Slow pyrolysis aims at the production of biochar, pyrolysis oil, and gases for various purposes, e.g., the production of H₂ [18–20]. Fast pyrolysis maximizes the yield of bio-oil, which is also known as pyrolysis oil. It employs high heating rates of 100 °C/s with temperatures between 450 °C and 550 °C and a residence time of 1 s [21–23].

The University of Twente (Thermal Engineering group) in the Netherlands has developed PyRos, which is a fast pyrolysis installation capable of processing approx. 30 kg/h of biomass. This reactor was patented with number WO0134725. PyRos is a cyclonic shaped type of reactor, and biomass is injected into the cyclone along with preheated inert material (sand) and gases. Centrifugal forces help in separating the solids from generated vapors and gases. Solids start sliding down the reactor walls. The biomass has direct contact with hot inert sand, which helps to achieve high heat transfer of the order of 500 up to 700 W/m²K. It also helps in a non-problematic in situ introduction of the catalyst. Produced chars find application in a fluidized bed combustor, generating the heat necessary for the process. CaO has been used as a catalyst in many different applications, such as oxidation of unburned pollutants in the flue gas [24], Fisher Tropsch synthesis [25], gasification [26], production of syngas from pyrolysis [27], and fast pyrolysis [22,28–30].

HTC is considered a thermal valorization process, typically performed at 200 to 260 °C in subcritical water at high pressure [31,32]. At temperatures of 200 up to 280 °C, the ionic constant of water increases significantly. Hence, water starts acting as a non-polar solvent [33,34]. The process generates a multitude of concurring reactions, yielding multiple types of products, especially with different types of biomass [31,32]. The first stage of the HTC process is hydrolysis, followed by dehydration as well as decarboxylation [35]. Dehydration results in decreasing the number of hydroxyl groups [31]. Decarboxylation promotes the formation of CO₂ [36,37]. A decrease in the amount of OH groups also results in a lower O/C ratio. Decarboxylation results in decreasing the amount of COOH and C=O groups, also slightly decreasing the O/C ratio of the solid product [31,38,39]. This is followed by further polymerization and aromatization [31,35]. The ability to decrease the O/C ratio is considered beneficial when valorization is performed, from the point of view of subsequent pyrolysis [40–42]. Due to these factors, HTC is considered one of a viable means of valorizing wet biomass before pyrolysis [43–45].

A decrease in the number of hydroxyl groups is considered one of the key aspects in making hydrothermally carbonized biomass more hydrophobic, resulting in lowering its equilibrium moisture content [46], making physical dewatering easier [47–50].

HTC increases the higher heating value (HHV) of the product (hydrochar) in comparison to the feedstock [51–53]. Moreover, the process of hydrothermal carbonization also removes a part of the inorganic fraction of biomass [54,55]. Hydrothermal carbonization also has an influence on the morphology of the hydrochars [56,57], and, as a consequence, makes the latter a good precursor for the production of activated carbon [58,59] and also for direct application to soil or compost [60,61]. Furthermore, positive influence of the HTC process on biomass grindability should not be overlooked, as particle size is an important aspect of pyrolysis [62–64].

Several studies on pyrolysis of HTC-treated materials could be found in the literature, including studies on kinetics [45], as well as studies focusing on the composition of pyrolysis oil/vapors [44,65] or studying both aspects [66,67]. However, looking at the heating rates applied within the scope of these studies, obtained values were not relevant for fast pyrolysis.

The goal of this work is to determine the effect that HTC treatment has on fuel properties of raw biomass, relevant from the point of view of fast pyrolysis, as well as to determine the influence of the treatment on fast pyrolysis kinetics, using a bespoke cyclonic TGA, and comparing it with the influence of an in-situ addition of a catalyst (CaO). Determination of kinetics at process conditions relevant to fast pyrolysis, as well as the

influence of HTC treatment and use of CaO on the kinetics of fast pyrolysis, is an important novelty of this work.

2. Materials and Methods

2.1. Feedstock and Hydrothermal Carbonization Experiments

The HTC experiments were performed at temperatures of 180, 200, and 220 °C with a residence time of 10 min and a water-to-biomass ratio of 12:1, in a pressure-tight vessel, with temperature measured using a K thermocouple (Figure 1). The heat was delivered to the reactor by immersing it in a hot fluidized bed. The level of immersion was used for controlling the temperature in the vessel by controlling the energy balance, i.e., the heat delivered and dissipated. The operator ensured that the temperature during the experiment did not deviate from the temperature selected for a particular experiment by more than 3.5 °C. Depending on the required temperature of HTC, the heating up period took between 3.5 and 9 min, with average heating rates ranging between 21 and 48 °C/min. After reaching the required temperature, the reactor was kept in the hot fluidized bed for 10 min and subsequently taken out for cooling. The reactor was initially cooled down using a cold fluidized bed, with air as a fluidizing agent, until reaching approximately 120 °C in order to quickly stop the process, which took between 6.5 and 14.5 min depending on the process temperature. After reaching this temperature, the reactor was transferred to cold water to reach room temperature. Cold solids were drained using a Buchner funnel after emptying the reactor and subsequently dried for 24 h at 105 °C. All experiments were carried out in triplicate.

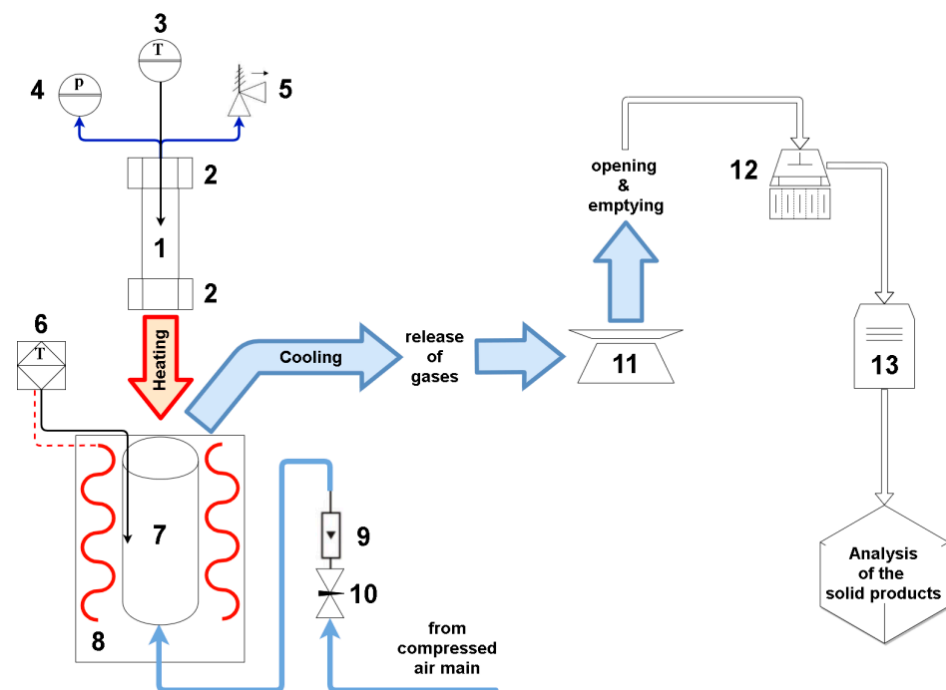


Figure 1. Hydrothermal carbonization test rig: 1—autoclave; 2—fittings able to withstand the pressure; 3—thermocouple; 4—pressure sensor; 5—safety valve; 6—thermocouple measuring the temperature inside of the hot fluidized bed; 7—fluidized bed used for heating the autoclave; 8—band heaters; 9—flow meter; 10—needle valve; 11—balance; 12—hydraulic press for dewatering; 13—oven for drying.

2.2. Cyclonic TGA

The cyclonic thermogravimeter (TGA) is a bespoke device developed by the University of Twente (Thermal Engineering group). The key element of this rig (Figure 2) is a heated cyclonic chamber, where devolatilization takes place. N₂ is pre-heated before being injected into the chamber in a tangential direction. The whole reactor is located on a very sensitive

balance, which measures mass loss over time. The balance itself consists of a high-speed damped load cell (Tedeia-Huntleigh, type 9010) in combination with a Penko QMA indicator. Flexible hoses were used for connections between the reactor, and other devices (N₂ supply and controls) were flexible to minimize their impact on the recorded weight. The temperature inside the reactor chamber was controlled by a programmable logic controller (PLC) and measured using K type thermocouple.

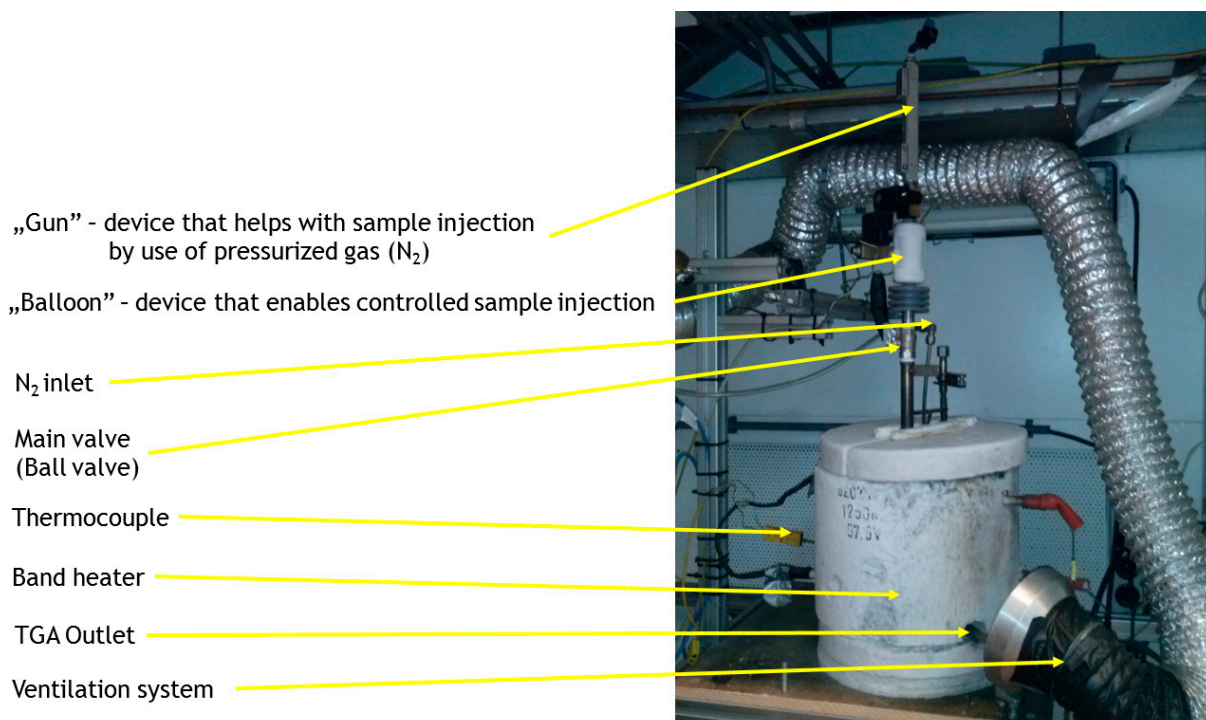


Figure 2. Cyclonic TGA.

The Cyclonic TGA was developed in order to determine pyrolysis kinetics at heating rates exceeding the possibilities of state-of-the-art analytical thermogravimetry since the heating rate has a significant influence on the kinetics of pyrolysis [68–71]. The setup was developed in order to ensure heating rates comparable to the fast pyrolysis process [72]. Its operating principle is similar to a fast pyrolysis reactor developed at the University of Twente (PyRos). In the reactor, solids slide down the walls while the processed biomass is in direct contact with hot inert sand ensuring heat transfer of 500–700 W/m²K [73]. This operating principle also ensures easy application of any catalyst in situ. Produced char is used in a fluidized bed combustor to obtain the heat necessary for the process [73,74]. Fast pyrolysis experiments were performed using Cyclonic TGA at temperatures between 450 °C and 500 °C, using sieved feedstock samples (miscanthus and hydrochars) with particle size ranging between 63 and 425 µm. Pyrolysis was performed in an inert atmosphere, with a majority of N₂ being pre-heated in the heated spiral pipe, inside of the thermal insulation of the reactor, and subsequently injected tangentially. A small volume of N₂ (approx. 100 mL at 3 bar pressure) was used for rapid injection of the sample into the cyclonic reactor. Blank trials with no sample have been performed in order to eliminate the effect of the inertia of injected gas, and short-time fluctuation of the scale has been deducted.

2.3. Characterization of Feedstock and Products

The miscanthus used for this study was obtained from Warsaw University of Life Sciences—SGGW in Skierniewice. Before HTC pre-treatment and characterization, the biomass was dried at 105 °C for one day and slashed into pieces with a size between 6 and 12 mm. Proximate analysis was performed using gravimetric methods. Ash content was determined by ashing samples at 815 °C for 4 h, whereas volatile matter content was

determined by holding crucibles with samples at 900 °C for 7 min. The calorimetric bomb (IKA C2000) was used for determining HHV. The C, H, N, and O content was determined using an elemental analyzer (Flash 2000, Thermo Scientific, Waltham, MA, USA). Samples with a particle size of less than 0.125 mm and a weight of approximately 0.5 mg were used for the analyses. All tests for proximate and ultimate analysis were performed in duplicates.

2.4. Analyses and Calculations

Reaction rate constants were obtained by fitting mass loss history to the function described by Equation (1), as follows [72]:

$$\frac{d\alpha}{dt} = k \cdot (1 - \alpha)^n \quad (1)$$

where:

- α —extent of reaction;
- t —reaction time, s;
- k —reaction rate constant, 1/s;
- n —order of the reaction.

The extent of the reaction is dimensionless and defined according to the formula [72]:

$$\alpha(t) = \frac{m_0 - m}{m_0 - m_f} \quad (2)$$

where:

- m_0 —initial solid mass, kg;
- m —mass at given time t , kg;
- m_f —solid mass after no more mass loss is observable (mass of char), kg.

Fitting was performed for α ranging between 0.25 and 0.7, assuming the order of reaction be equal to one. Subsequently, the kinetic triplet was determined using the Arrhenius plot, assuming that the global kinetic constant follows the Arrhenius rate law [72,75]:

$$k = A \cdot e^{\left(-\frac{E_a}{R \cdot T}\right)} \quad (3)$$

where:

- k —reaction rate constant, 1/s;
- E_a —activation energy, J/mol;
- R —universal gas constant, J/mol·K;
- T —temperature, K.

The mass yield (Y_m) and energy yield (Y_e) are typically used for the assessment of the performance of thermal valorization processes [76,77]. Y_m was assessed using a direct method according to the following equation:

$$Y_m = \frac{m_{prod-dry}}{m_{feedst-dry}} \quad (4)$$

where:

- $m_{prod-dry}$ —dry mass of the product (hydrochar);
- $m_{feedst-dry}$ —dry mass of the feedstock.

The energy yield was calculated using following equation [78–80]:

$$Y_e = Y_m \cdot \frac{HHV_{product}}{HHV_{feedstock}} \quad (5)$$

where:

- Y_e —energy yield, -;
- HHV —higher heating value, MJ/kg.

Ash yield, as defined by Mościcki et al. [32], has been used for assessing the fraction of inorganics that remained in hydrochars after the HTC process, with respect to the inorganic fraction of the feedstock:

$$Y_a = Y_m \cdot \frac{A_{product}}{A_{feedstock}} \quad (6)$$

where:

Y_a —ash yield, -;

A —ash content, dry basis, %_{db}.

3. Results and Discussion

3.1. Hydrothermal Carbonization—Process Performance and Effect of HTC Treatment on Valorized Miscanthus

Mass yields (Figure 3) obtained during the experimental investigation performed within the scope of this work were higher in comparison to results reported by the literature for HTC of miscanthus. Mihajlović et al. [81] reported mass yields of 73%, 54%, and 51% for HTC of miscanthus at 180 °C, 200 °C, and 220 °C, respectively. The residence time of HTC was 60 min for the aforementioned study [81]. Similarly, Smith et al. [55] obtained a mass yield of approximately 58% for HTC of miscanthus at 200 °C, with a residence time of one hour. The same study reported a mass yield of approximately 40% for HTC of miscanthus at 250 °C, also performed with a residence time of one hour [82]. Wilk and Magdziarz [82] reported a mass yield of 80% for HTC of miscanthus at 180 °C, with a residence time of 4 h. The same study reported mass yields ranging between 65% and 63% for HTC of miscanthus at 200 °C, with residence times ranging between 2 and 12 h [82]. This suggests that for HTC of miscanthus residence times longer than two hours do not have any significant influence on the mass yield, and are not justified since the process is finished before that time. On the other hand, mass yields obtained in this study were much higher. This is well explained by the residence time of 10 min used for this study. Similar mass yields have been reported for HTC of miscanthus by other studies, where shorter residence times were applied. For instance, Kambo and Dutta [83] reported mass yields for HTC of miscanthus at 190 °C ranging between 82.8% and 66.6% for residence times between 5 and 30 min. Similarly, Toufiq Reza et al. [84] reported a mass yield of 79% for HTC of miscanthus at 200 °C, with a residence time of 5 min. Small differences between Y_m reported by studies performed with short residence times and this study could be attributed mainly to heating rates and, as a consequence, heating-up time for the reactor, as well as cooling-down times. The study of Toufiq Reza et al. [84] did not report either the heating up time or heating rate and only reported that the cooling was obtained by immersing the reactor in an ice bath. On the other hand, the study of Kambo and Dutta [83] reported that it took 20 to 30 min for their reactor to achieve desired temperatures. The same study also reported cooling down in cold water, taking between 5 and 7 min [83]. Since both studies used similar reactors, produced by Parr and controlled by a PID controller, it seems plausible that also, in the case of experiments performed by Toufiq Reza et al. [84], similar time was needed to heat up the reactor to desired temperature. This is much higher than the heating up times in this study (3.5 to 9 min), suggesting lower average heating rates achieved by Toufiq Reza et al. [84]. In such circumstances, it seems plausible to use this as an explanation of achieving higher Y_m by this study, especially for HTC at 180 °C, for which it took only 3.5 min to reach the desired temperature by the reactor, in comparison to 20 min for Kambo and Dutta [83]. It is clear, when looking at the trend shown in Figure 3, that the HTC process starts at temperatures lower than 180 °C, since the trend line reaches $Y_m = 1$ for the temperatures slightly lower than 170 °C. This is in good qualitative agreement with the work of Funke and Ziegler, reporting carboxyl and carbonyl groups in biomass degrading above 150 °C [31], and small deviation could be explained by the specifics of the feedstock in this particular study, as well as by the fact that 3.5 °C tolerance for the temperature, controlled manually, to some extent influenced the results, thus indirectly influencing the slope of the trend line in Figure 3.

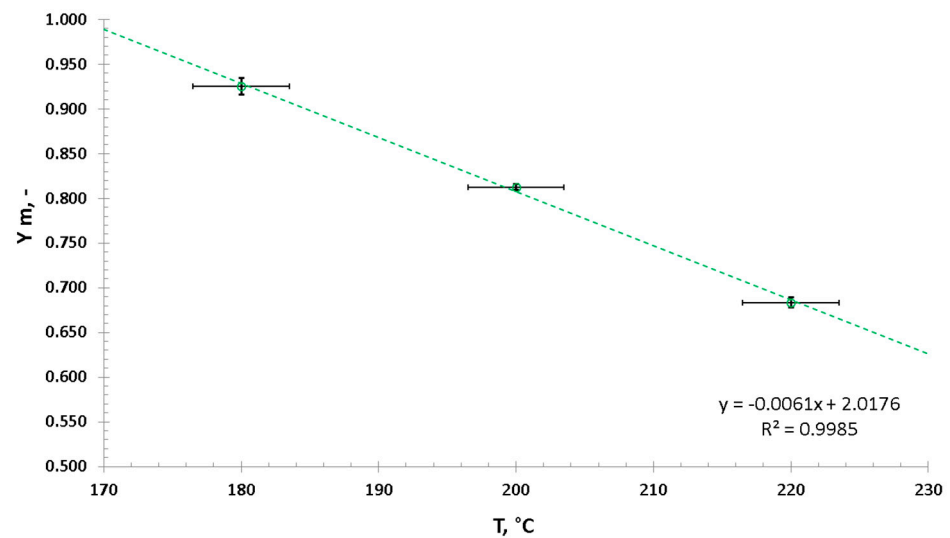


Figure 3. Mass yield for the performed HTC experiments.

Energy yields, shown in Figure 4, are higher than respective mass yields, which is caused by the fact that Y_e is the result of the multiplication of Y_m by respective energy densification ratio (ED) [85,86]. Interestingly, the slope for Y_m is much steeper than the slope for Y_e , implying a more extensive difference between Y_m and Y_e for higher HTC temperatures, thus implying ED increases with higher temperatures of the HTC process. This has been confirmed by many studies [87–89]. For both Y_m (Figure 3) and Y_e (Figure 4), the best fit was achieved by a linear function.

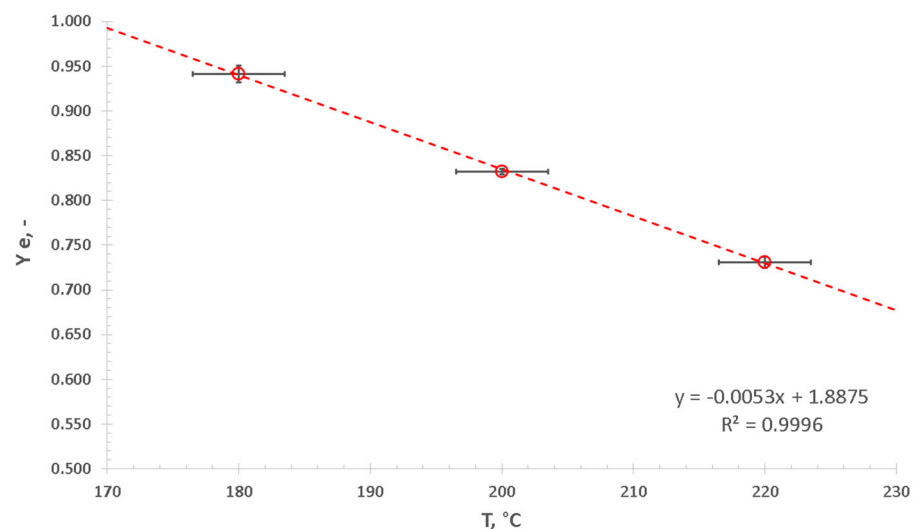


Figure 4. Energy yield for the performed HTC experiments.

On the other hand, the best fit for ash yield (Figure 5) was achieved using a 2nd-order polynomial. Moreover, the polynomial reaches values close to 1.0 at temperatures below 100 °C. This seems sensible since $Y_a < 1$ indicates that a part of the inorganic content of raw biomass was washed out during the treatment, and it has been reported in the literature that washing biomass with hot water can remove a part of its ash [90,91].

Overall, HTC treatment led to a decrease in volatile matter content and a simultaneous increase in fixed carbon content (Figure 6), which is typical for HTC of many different types of biomass, as reported in the literature [92]. Moreover, according to expectations, HTC treatment led to an increase in higher heating value (HHV), as shown in Figure 7, which has also been reported in the literature [93,94].

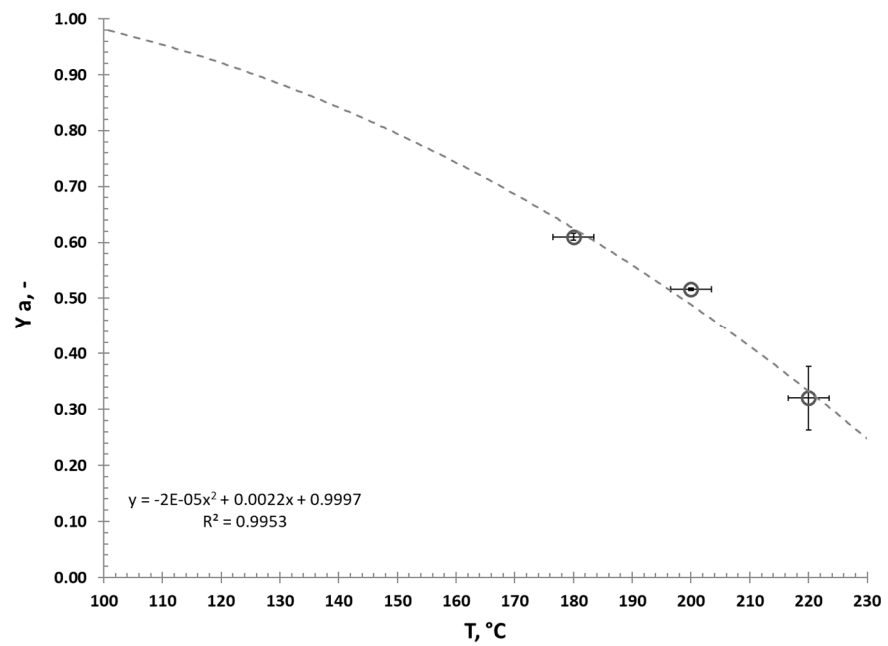


Figure 5. Ash yield for the performed HTC experiments.

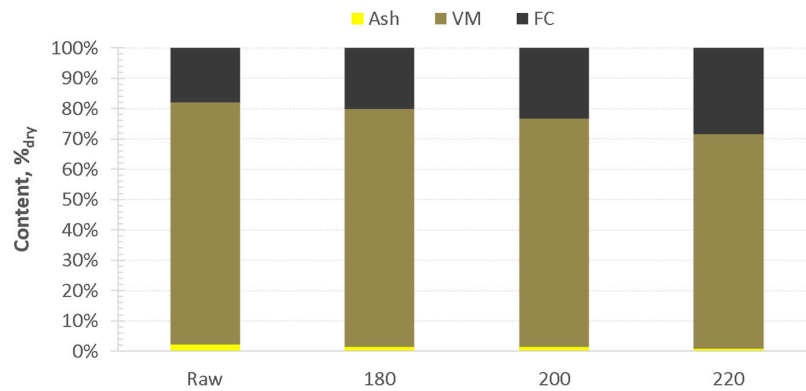


Figure 6. Proximate analysis of the raw sample, before HTC, and hydrochars obtained at respective temperatures.

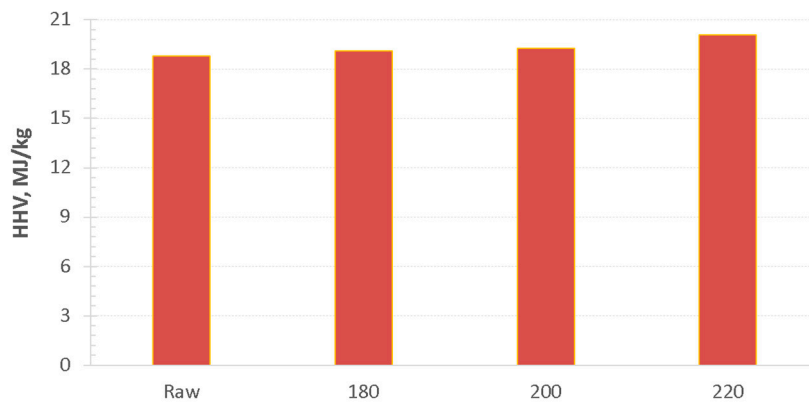


Figure 7. Higher heating values of the raw sample, before HTC, and hydrochars obtained at respective temperatures.

HTC of miscanthus, in line with the expectations, led to an increase in carbon content and a simultaneous decrease in the oxygen content of the valorized samples on a dry ash-free basis (Figure 8), when compared to the raw biomass. Since HHV and C content

are strongly correlated [95,96], this is a good explanation of the observed HHV increase (Figure 7). A decrease in the oxygen content seems to be beneficial in terms of subsequent pyrolysis of such materials since it has been reported in the literature that high oxygen content of biomass has a detrimental influence on the quality of pyrolysis oil, including parameters such as pH and viscosity [23,74], thus influencing combustion as well as injection and atomization properties of the pyrolysis oil [97,98].

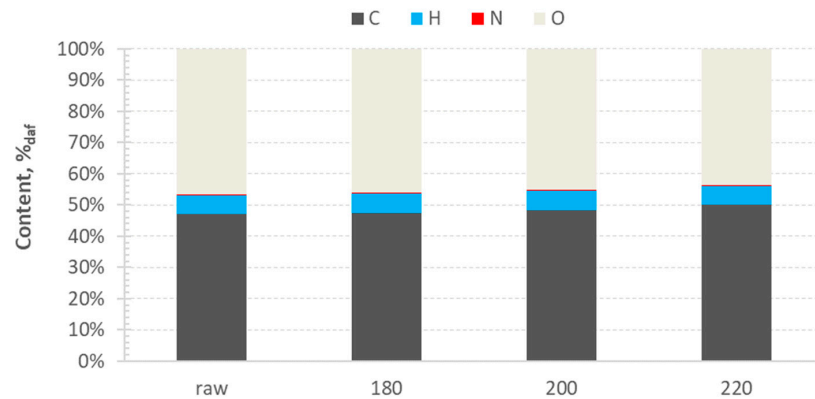


Figure 8. Ultimate analysis of the raw sample, before HTC, and hydrochars obtained at respective temperatures.

Van Krevelen's diagram (Figure 9) shows clearly that the HTC process resembles the natural process of coalification, judging by the trend and respective location of raw miscanthus and hydrochars obtained at different temperatures, with respect to peat, lignite, and hard coal. The hydrochars were still in the typical area of biomass [88,99–102]. However, what needs to be taken into account is the initial location of the raw miscanthus. A similar carbonization trend has been reported for HTC-treated miscanthus by Wilk and Magdziarz [82], where some of the samples, namely, HTC-treated at 220 °C, were located in the typical area for peat. However, the treatment time for the aforementioned hydrochar was 4 h [82], which is much longer than the 10 min applied in this study.

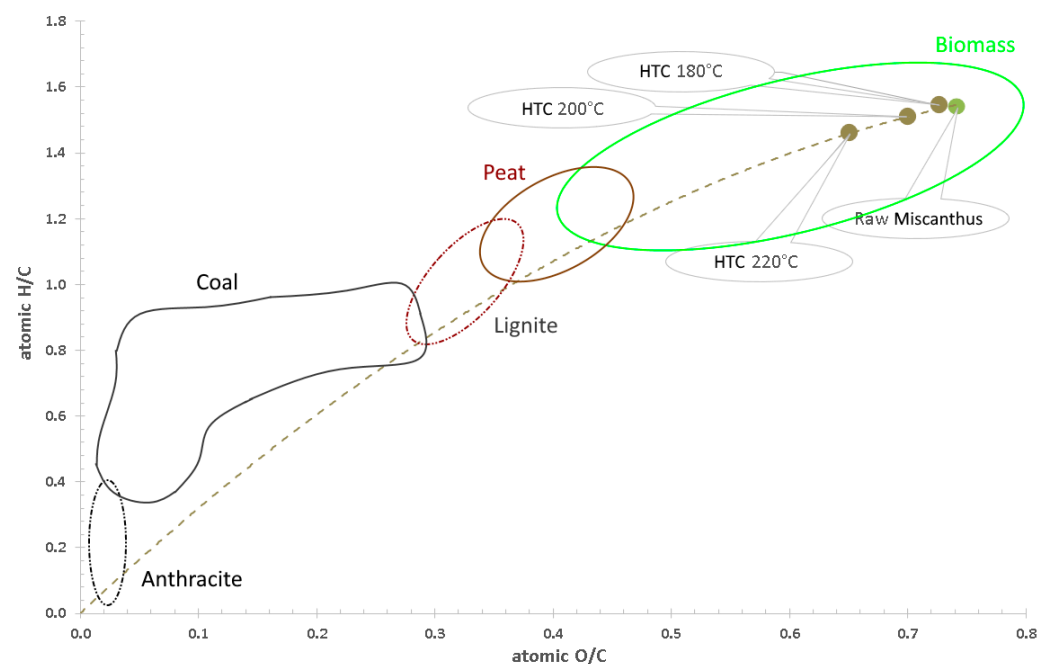


Figure 9. Van Krevelen's diagram for the raw sample, before HTC, and hydrochars obtained at respective temperatures (locations of different solid fuels adapted from [103–108]).

3.2. Fast Pyrolysis Kinetics—Influence of HTC and CaO Addition

It could be clearly seen from the Arrhenius plot (Figure 10) that HTC treatment exerted its influence on the kinetics of fast pyrolysis of miscanthus. In general, the inclination of the slope was higher for HTC-treated samples in comparison to the raw biomass. The effect was comparable to the effect made by CaO addition (as shown in Figure 11). Looking at Figure 11, the in situ addition of 20% of CaO catalyst allowed for achieving similar kinetics as for pyrolysis of the raw miscanthus. Other studies using CaO as an in situ catalyst in different types of fluidized beds and fixed beds had even higher mass shares of CaO, reaching Ca to biomass ratios as high as 2:1 [26]. However, the important difference is that the catalyst added in this study was initially cold and needed to be heated up after injection with biomass, locally decreasing the temperature at the beginning of the process. Nonetheless, despite such a limitation, activation energies determined within the scope of this study (Table 1) were much lower than the values reported for slow pyrolysis of miscanthus by Mlonka-Mędrala et al. [109].

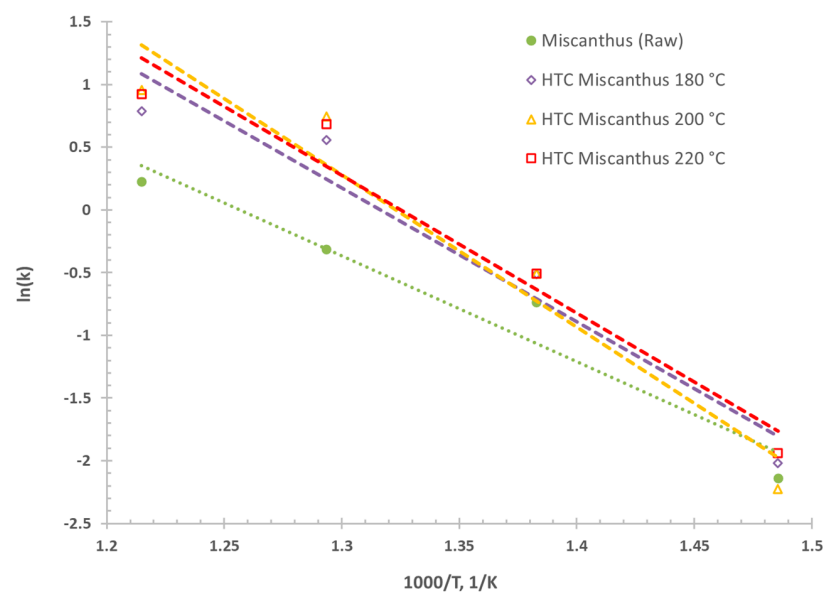


Figure 10. Arrhenius plot for pyrolysis of Miscanthus—influence of HTC (dotted lines are trend lines).

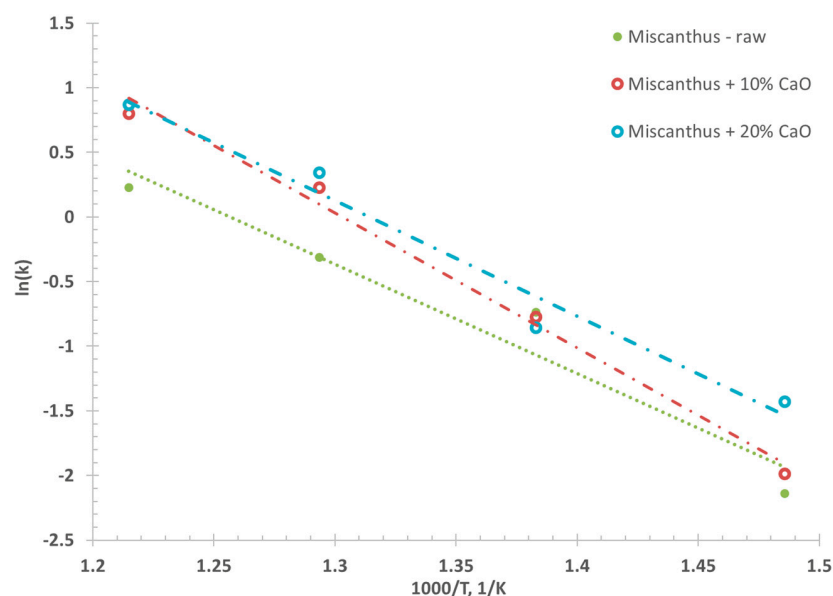


Figure 11. Arrhenius plot for pyrolysis of Miscanthus—influence of catalyst (dotted lines are trend lines).

Table 1. Activation energy and pre-exponential (frequency) factor for fast pyrolysis of Miscanthus.

	R ²	E_a	ln A	A	
		kJ/mol	1/s	1/s	1/min
Miscanthus (Raw)	0.9454	70.25	10.619	4.09×10^4	6.82×10^2
Miscanthus + 10% CaO	0.9909	86.75	13.594	8.01×10^5	1.34×10^4
Miscanthus + 20% CaO	0.9717	74.48	11.774	1.30×10^5	2.16×10^3
HTC Miscanthus 180 °C	0.9452	88.83	14.064	1.28×10^6	2.14×10^4
HTC Miscanthus 200 °C	0.9399	101.10	16.087	9.69×10^6	1.62×10^5
HTC Miscanthus 220 °C	0.9530	91.33	14.556	2.10×10^6	3.49×10^4

Mlonka-Mędrala et al. [109] reported activation energies (E_a) for slow pyrolysis of miscanthus, performed at heating rates of 10 to 50 °C/min, using TGA in a non-isothermal regime, for temperatures up to 600 °C. Reported E_a were 175.64 and 177.02 kJ/mol for samples milled using a knife mill (with a sieving screen of 425 µm aperture) and roller mill, respectively [109]. Kumar et al. [110] reported the average E_a for pyrolysis of miscanthus, to be as high as 197.66 kJ/mol and 179.64 kJ/mol, using the KAS (Kissinger–Akahira–Sunose) and Starink methods, respectively. Heating rates ranging between 10 and 30 °C/min were used in this particular study [110]. Matusiak et al. [111] investigated the pyrolysis kinetics of miscanthus, applying heating rates of 5, 10, and 20 °C/min, and for the degree of conversion <0.8 obtained E_a ranging between 141.7 and 202.3 kJ/mol using Friedman's method [111]. For the Ozawa–Flynn–Wall method, the same study reported E_a ranging between 153.5 and 190.5 kJ/mol [111].

E_a values reported in this study (Table 1) were smaller than 101.10 kJ/mol for all the samples, indicating the importance of the heating rates of the process. Higher values of E_a were achieved for hydrochars and the CaO addition in comparison to pyrolysis of raw miscanthus. This is not surprising, as a part of the volatile matter is lost during the HTC process, as shown in Figure 6. Nonetheless, it is worth noting that the addition of 20% of CaO allowed for achieving almost the same value of E_a as for raw miscanthus (Table 1).

The results obtained within the scope of this study are in good qualitative agreement with the work of Cortes and Bridgewater [112]. The work reported E_a for pyrolysis of miscanthus, ranging between 129–156 kJ/mol, increased after acid hydrolysis treatment, reaching 200–376 kJ/mol [112]. Cortes and Bridgewater [112] performed pyrolysis at heating rates of 2.5, 5, 10, 17, and 25 °C/min. Therefore, the importance of the heating rates should not be overlooked, especially if fast pyrolysis is a subject of consideration. Moreover, similar qualitative confirmation of the trend of increasing E_a with hydrothermal pretreatment could be found in the work of Liu et al. [66], which showed that HTC pretreatment increased E_a in comparison to pyrolysis of untreated sewage sludge, with a heating rate of 10 °C/min [66].

Overall, the determination of the kinetics of pyrolysis is just a first step, allowing the optimization of the design of the pyrolysis reactor with respect to the residence time of biomass in the reactor, assuring desired conversion and, at the same time, separating the char as soon as possible, prior to quenching of the pyrolysis oil, thus achieving high oil yields, typical for fast pyrolysis. In the PyRos reactor, the separation of char is performed by the use of a Rotating Particle Separator prior to quenching [73,113]. However, further studies should be performed, assessing the effect of HTC treatment and the use of in situ catalyst on the quality and amounts of obtained pyrolysis oil, which is important for the performance of fast pyrolysis technology.

4. Conclusions

In general, hydrothermal carbonization influences subsequent fast pyrolysis in a couple of ways: firstly, a positive influence is the decrease in oxygen content as a result of HTC; this causes the presence of fewer oxygen-containing compounds in the pyrolysis oil, which are responsible for the poor characteristics of the pyrolysis oil as a liquid fuel.

Secondly, a part of inorganics is removed since an ash yield smaller than 1.0 is typically achieved, even for low residence times in HTC. This is important mainly due to the potentially detrimental influence of inorganics on the combustion properties of the solid residues (char), which is necessary for generating the heat required for fast pyrolysis. In many fast pyrolysis units, such combustion is performed in a fluidized bed, where agglomeration of the bed could be an important issue. Furthermore, improved grindability should be named as an important factor in favor of HTC as a pretreatment method for fast pyrolysis. However, this comes at a price of smaller quantities of volatiles available for pyrolysis, as a part of volatile matter is removed during HTC. An increase in activation energy of pyrolysis has been observed as a consequence of HTC treatment. Activation energy also decreased with an increasing share of the CaO catalyst. Further research should involve confirmation of the positive effects of HTC and addition of the catalyst on the properties of pyrolysis oil.

Author Contributions: Conceptualization: E.B., A.P., P.O. and G.B.; methodology: A.B., E.B. and P.O.; validation: H.P.-K., K.M. and A.A.; formal analysis: L.N. and A.B.; investigation: L.N., K.M. and M.W.; resources: E.B., A.P. and G.B.; data curation: K.M.; writing—original draft preparation: L.N., V., C.A.-B. and M.W.; writing—review and editing: L.N., A.A. and A.P.; visualization: L.N.; supervision: K.M., E.B., A.P., P.O. and G.B.; project administration: E.B., A.P., K.M. and L.N.; funding acquisition: L.N. All authors have read and agreed to the published version of the manuscript.

Funding: Financial support of this work from the National Science Centre, Poland—project no. 2019/33/N/ST8/02641, is gratefully acknowledged.

Institutional Review Board Statement: Not applicable.

Informed Consent Statement: Not applicable.

Data Availability Statement: Not applicable.

Conflicts of Interest: The authors declare no conflict of interest.

References

1. Tzelepi, V.; Zeneli, M.; Kourkoumpas, D.S.; Karampinis, E.; Gypakis, A.; Nikolopoulos, N.; Grammelis, P. Biomass Availability in Europe as an Alternative Fuel for Full Conversion of Lignite Power Plants: A Critical Review. *Energies* **2020**, *13*, 3390. [\[CrossRef\]](#)
2. Knapczyk, A.; Francik, S.; Jewiarz, M.; Zawisłak, A.; Francik, R. Thermal Treatment of Biomass: A Bibliometric Analysis—The Torrefaction Case. *Energies* **2020**, *14*, 162. [\[CrossRef\]](#)
3. Szufa, S.; Piersa, P.; Junga, R.; Błaszczuk, A.; Modliński, N.; Sobek, S.; Marczak-Grzesik, M.; Adrian, L.; Dzikuć, M. Numerical Modeling of the Co-Firing Process of an in Situ Steam-Torrefied Biomass with Coal in a 230 MW Industrial-Scale Boiler. *Energy* **2023**, *263*, 125918. [\[CrossRef\]](#)
4. Kopczyński, M.; Lasek, J.A.; Iluk, A.; Zuwała, J. The Co-Combustion of Hard Coal with Raw and Torrefied Biomasses (Willow (*Salix viminalis*), Olive Oil Residue and Waste Wood from Furniture Manufacturing). *Energy* **2017**, *140*, 1316–1325. [\[CrossRef\]](#)
5. Jian, J.; Lu, Z.; Yao, S.; Li, Y.; Liu, Z.; Lang, B.; Chen, Z. Effects of Thermal Conditions on Char Yield and Char Reactivity of Woody Biomass in Stepwise Pyrolysis. *J. Anal. Appl. Pyrolysis* **2019**, *138*, 211–217. [\[CrossRef\]](#)
6. Luo, H.; Lu, Z.; Jensen, P.A.; Glarborg, P.; Lin, W.; Dam-Johansen, K.; Wu, H. Experimental and Modelling Study on the Influence of Wood Type, Density, Water Content, and Temperature on Wood Devolatilization. *Fuel* **2020**, *260*, 116410. [\[CrossRef\]](#)
7. Wang, S.; Mandfloen, P.; Jönsson, P.; Yang, W. Synergistic Effects in the Copyrolysis of Municipal Sewage Sludge Digestate and Salix: Reaction Mechanism, Product Characterization and Char Stability. *Appl. Energy* **2021**, *289*, 116687. [\[CrossRef\]](#)
8. Zaini, I.N.; Wen, Y.; Mousa, E.; Jönsson, P.G.; Yang, W. Primary Fragmentation Behavior of Refuse Derived Fuel Pellets during Rapid Pyrolysis. *Fuel Process. Technol.* **2021**, *216*, 106796. [\[CrossRef\]](#)
9. Kantorek, M.; Jesionek, K.; Polesek-Karczewska, S.; Ziółkowski, P.; Stajnke, M.; Badur, J. Pilot Installation for Thermal Utilization of Meat-and-Bone Meal Using the Rotary Kiln Pyrolyzer and the Fluidised Bed Boiler. *E3S Web Conf.* **2019**, *137*, 01013. [\[CrossRef\]](#)
10. Kantorek, M.; Jesionek, K.; Polesek-Karczewska, S.; Ziółkowski, P.; Stajnke, M.; Badur, J. Thermal Utilization of Meat-and-Bone Meal Using the Rotary Kiln Pyrolyzer and the Fluidized Bed Boiler—The Performance of Pilot-Scale Installation. *Renew. Energy* **2021**, *164*, 1447–1456. [\[CrossRef\]](#)
11. Čespiva, J.; Jadlovec, M.; Výtisk, J.; Serenčíšová, J.; Tadeáš, O.; Honus, S. Softwood and Solid Recovered Fuel Gasification Residual Chars as Sorbents for Flue Gas Mercury Capture. *Environ. Technol. Innov.* **2023**, *29*, 102970. [\[CrossRef\]](#)
12. Szul, M.; Iluk, T.; Zuwała, J. Use of CO₂ in Pressurized, Fluidized Bed Gasification of Waste Biomasses. *Energies* **2022**, *15*, 1395. [\[CrossRef\]](#)

13. Sieradzka, M.; Mlonka-Mędrala, A.; Magdziarz, A. Comprehensive Investigation of the CO₂ Gasification Process of Biomass Wastes Using TG-MS and Lab-Scale Experimental Research. *Fuel* **2022**, *330*, 125566. [[CrossRef](#)]
14. Szufa, S.; Dzikuć, M.; Adrian, Ł.; Piersa, P.; Romanowska-Duda, Z.; Lewandowska, W.; Marcza, M.; Błaszczuk, A.; Piwowar, A. Torrefaction of Oat Straw to Use as Solid Biofuel, an Additive to Organic Fertilizers for Agriculture Purposes and Activated Carbon—TGA Analysis, Kinetics. *E3S Web Conf.* **2020**, *154*, 02004. [[CrossRef](#)]
15. Kerdsuwan, S.; Laohalidanond, K.; Gupta Ashwani, K. Upgrading Refuse-Derived Fuel Properties from Reclaimed Landfill Using Torrefaction. *J. Energy Resour. Technol.* **2021**, *143*, 021302. [[CrossRef](#)]
16. Piersa, P.; Szufa, S.; Czerwińska, J.; Ünyay, H.; Adrian, Ł.; Wielgosinski, G.; Obraniak, A.; Lewandowska, W.; Marczak-Grzesik, M.; Dzikuć, M.; et al. Pine Wood and Sewage Sludge Torrefaction Process for Production Renewable Solid Biofuels and Biochar as Carbon Carrier for Fertilizers. *Energies* **2021**, *14*, 8176. [[CrossRef](#)]
17. Lasek, J.A.; Kopczyński, M.; Janusz, M.; Iluk, A.; Zuwała, J. Combustion Properties of Torrefied Biomass Obtained from Flue Gas-Enhanced Reactor. *Energy* **2017**, *119*, 362–368. [[CrossRef](#)]
18. Piersa, P.; Unyay, H.; Szufa, S.; Lewandowska, W.; Modrzewski, R.; Ślęzak, R.; Ledakowicz, S. An Extensive Review and Comparison of Modern Biomass Torrefaction Reactors vs. Biomass Pyrolysis—Part 1. *Energies* **2022**, *15*, 2227. [[CrossRef](#)]
19. Wen, Y.; Wang, S.; Shi, Z.; Nuran Zaini, I.; Niedzwiecki, L.; Aragon-Briceno, C.; Tang, C.; Pawlak-Kruczek, H.; Jönsson, P.G.; Yang, W. H₂-Rich Syngas Production from Pyrolysis of Agricultural Waste Digestate Coupled with the Hydrothermal Carbonization Process. *Energy Convers. Manag.* **2022**, *269*, 116101. [[CrossRef](#)]
20. Wang, S.; Wen, Y.; Shi, Z.; Niedzwiecki, L.; Baranowski, M.; Czerep, M.; Mu, W.; Kruczek, H.P.; Jönsson, P.G.; Yang, W. Effect of Hydrothermal Carbonization Pretreatment on the Pyrolysis Behavior of the Digestate of Agricultural Waste: A View on Kinetics and Thermodynamics. *Chem. Eng. J.* **2022**, *431*, 133881. [[CrossRef](#)]
21. Jahirul, M.I.; Rasul, M.G.; Chowdhury, A.A.; Ashwath, N. Biofuels Production through Biomass Pyrolysis—A Technological Review. *Energies* **2012**, *5*, 4952–5001. [[CrossRef](#)]
22. Mysore Prabhakara, H.; Bramer, E.A.; Brem, G. Role of Dolomite as an In-Situ CO₂ Sorbent and Deoxygenation Catalyst in Fast Pyrolysis of Beechwood in a Bench Scale Fluidized Bed Reactor. *Fuel Process. Technol.* **2021**, *224*, 107029. [[CrossRef](#)]
23. Bridgwater, A.V. Review of Fast Pyrolysis of Biomass and Product Upgrading. *Biomass Bioenergy* **2012**, *38*, 68–94. [[CrossRef](#)]
24. Ryšavý, J.; Horák, J.; Hopan, F.; Kuboňová, L.; Krpec, K.; Molchanov, O.; Garba, M.; Ochodek, T. Influence of Flue Gas Parameters on Conversion Rates of Honeycomb Catalysts. *Sep. Purif. Technol.* **2021**, *278*, 119491. [[CrossRef](#)]
25. Čespiva, J.; Skřínský, J.; Vereš, J.; Borovec, K.; Wnukowski, M. Solid-Recovered Fuel to Liquid Conversion Using Fixed Bed Gasification Technology and a Fischer–Tropsch Synthesis Unit—Case Study. *Int. J. Energy Prod. Manag.* **2020**, *5*, 212–222. [[CrossRef](#)]
26. Li, H.; Wang, Y.; Zhou, N.; Dai, L.; Deng, W.; Liu, C.; Cheng, Y.; Liu, Y.; Cobb, K.; Chen, P.; et al. Applications of Calcium Oxide–Based Catalysts in Biomass Pyrolysis/Gasification—A Review. *J. Clean. Prod.* **2021**, *291*, 125826. [[CrossRef](#)]
27. Yang, S.; Zhang, X.; Chen, L.; Sun, L.; Xie, X.; Zhao, B. Production of Syngas from Pyrolysis of Biomass Using Fe/CaO Catalysts: Effect of Operating Conditions on the Process. *J. Anal. Appl. Pyrolysis* **2017**, *125*, 1–8. [[CrossRef](#)]
28. Sun, L.; Zhang, X.; Chen, L.; Xie, X.; Yang, S.; Zhao, B.; Si, H. Effect of Preparation Method on Structure Characteristics and Fast Pyrolysis of Biomass with Fe/CaO Catalysts. *J. Anal. Appl. Pyrolysis* **2015**, *116*, 183–189. [[CrossRef](#)]
29. Vichaphund, S.; Sricharoenchaikul, V.; Atong, D. Industrial Waste Derived CaO-Based Catalysts for Upgrading Volatiles during Pyrolysis of Jatropha Residues. *J. Anal. Appl. Pyrolysis* **2017**, *124*, 568–575. [[CrossRef](#)]
30. Echresh Zadeh, Z.; Abdulkhani, A.; Saha, B. A Comparative Production and Characterisation of Fast Pyrolysis Bio-Oil from Populus and Spruce Woods. *Energy* **2021**, *214*, 118930. [[CrossRef](#)]
31. Funke, A.; Ziegler, F. Hydrothermal Carbonisation of Biomass: A Summary and Discussion of Chemical Mechanisms for Process Engineering. *Biofuels Bioprod. Biorefining* **2010**, *4*, 160–177. [[CrossRef](#)]
32. Moscicki, K.J.; Niedzwiecki, L.; Owczarek, P.; Wnukowski, M. Commoditization of Wet and High Ash Biomass: Wet Torrefaction—A Review. *J. Power Technol.* **2017**, *97*, 354–369.
33. Jackowski, M.; Semba, D.; Trusek, A.; Wnukowski, M.; Niedzwiecki, L.; Baranowski, M.; Krochmalny, K.; Pawlak-Kruczek, H. Hydrothermal Carbonization of Brewery’s Spent Grains for the Production of Solid Biofuels. *Beverages* **2019**, *5*, 12. [[CrossRef](#)]
34. Peterson, A.A.; Vogel, F.; Lachance, R.P.; Fröling, M.; Antal, M.J.; Tester, J.W. Thermochemical Biofuel Production in Hydrothermal Media: A Review of Sub- and Supercritical Water Technologies. *Energy Environ. Sci.* **2008**, *1*, 32–65. [[CrossRef](#)]
35. Reza, M.T.; Andert, J.; Wirth, B.; Busch, D.; Pielert, J.; Lynam, J.G.; Mumme, J. Hydrothermal Carbonization of Biomass for Energy and Crop Production. *Appl. Bioenergy* **2014**, *1*, 11–29. [[CrossRef](#)]
36. Picone, A.; Volpe, M.; Messineo, A. Process Water Recirculation during Hydrothermal Carbonization of Waste Biomass: Current Knowledge and Challenges. *Energies* **2021**, *14*, 2962. [[CrossRef](#)]
37. Calucci, L.; Forte, C. Influence of Process Parameters on the Hydrothermal Carbonization of Olive Tree Trimmings: A 13C Solid-State NMR Study. *Appl. Sci.* **2023**, *13*, 1515. [[CrossRef](#)]
38. Satira, A.; Paone, E.; Bressi, V.; Iannazzo, D.; Marra, F.; Calabrò, P.S.; Mauriello, F.; Espro, C. Hydrothermal Carbonization as Sustainable Process for the Complete Upgrading of Orange Peel Waste into Value-Added Chemicals and Bio-Carbon Materials. *Appl. Sci.* **2021**, *11*, 10983. [[CrossRef](#)]

39. González, R.; Ellacuriaga, M.; Aguilar-Pesantes, A.; Carrillo-Peña, D.; García-Cascallana, J.; Smith, R.; Gómez, X. Feasibility of Coupling Anaerobic Digestion and Hydrothermal Carbonization: Analyzing Thermal Demand. *Appl. Sci.* **2021**, *11*, 11660. [[CrossRef](#)]
40. Louwes, A.C.; Basile, L.; Yukananto, R.; Bhagwandas, J.C.; Bramer, E.A.; Brem, G. Torrefied Biomass as Feed for Fast Pyrolysis: An Experimental Study and Chain Analysis. *Biomass Bioenergy* **2017**, *105*, 116–126. [[CrossRef](#)]
41. Sieradzka, M.; Gao, N.; Quan, C.; Mlonka-Mędrala, A.; Magdziarz, A. Biomass Thermochemical Conversion via Pyrolysis with Integrated CO₂ Capture. *Energies* **2020**, *13*, 1050. [[CrossRef](#)]
42. Kantorek, M.; Jesionek, K.; Polesek-Karczewska, S.; Ziółkowski, P.; Badur, J. Thermal Utilization of Meat and Bone Meals. Performance Analysis in Terms of Drying Process, Pyrolysis and Kinetics of Volatiles Combustion. *Fuel* **2019**, *254*, 115548. [[CrossRef](#)]
43. Wang, S.; Yang, H.; Shi, Z.; Zaini, I.N.; Wen, Y.; Jiang, J.; Jönsson, P.G.; Yang, W. Renewable Hydrogen Production from the Organic Fraction of Municipal Solid Waste through a Novel Carbon-Negative Process Concept. *Energy* **2022**, *252*, 124056. [[CrossRef](#)]
44. Magdziarz, A.; Wilk, M.; Wądrzyk, M. Pyrolysis of Hydrochar Derived from Biomass—Experimental Investigation. *Fuel* **2020**, *267*, 117246. [[CrossRef](#)]
45. Duan, Y.; Ning, Y.; Gao, N.; Quan, C.; Grammelis, P.; Boutikos, P. Effect of Hydrothermal Process on the Pyrolysis of Oily Sludge: Characterization and Analysis of Pyrolysis Products. *Fuel* **2023**, *338*, 127347. [[CrossRef](#)]
46. Acharjee, T.C.; Coronella, C.J.; Vasquez, V.R. Effect of Thermal Pretreatment on Equilibrium Moisture Content of Lignocellulosic Biomass. *Bioresour. Technol.* **2011**, *102*, 4849–4854. [[CrossRef](#)] [[PubMed](#)]
47. Ahmed, M.; Andreottola, G.; Elagroudy, S.; Negm, M.S.; Fiori, L. Coupling Hydrothermal Carbonization and Anaerobic Digestion for Sewage Digestate Management: Influence of Hydrothermal Treatment Time on Dewaterability and Bio-Methane Production. *J. Environ. Manag.* **2021**, *281*, 111910. [[CrossRef](#)] [[PubMed](#)]
48. Gao, N.; Li, Z.; Quan, C.; Miskolczi, N.; Egedy, A. A New Method Combining Hydrothermal Carbonization and Mechanical Compression In-Situ for Sewage Sludge Dewatering: Bench-Scale Verification. *J. Anal. Appl. Pyrolysis* **2019**, *139*, 187–195. [[CrossRef](#)]
49. Wang, L.-F.; Qian, C.; Jiang, J.-K.; Ye, X.-D.; Yu, H.-Q. Response of Extracellular Polymeric Substances to Thermal Treatment in Sludge Dewatering Process. *Environ. Pollut.* **2017**, *231*, 1388–1392. [[CrossRef](#)] [[PubMed](#)]
50. Wang, L.; Zhang, L.; Li, A. Hydrothermal Treatment Coupled with Mechanical Expression at Increased Temperature for Excess Sludge Dewatering: Influence of Operating Conditions and the Process Energetics. *Water Res.* **2014**, *65*, 85–97. [[CrossRef](#)]
51. Ruiz, H.A.; Rodríguez-Jasso, R.M.; Fernandes, B.D.; Vicente, A.A.; Teixeira, J.A. Hydrothermal Processing, as an Alternative for Upgrading Agriculture Residues and Marine Biomass according to the Biorefinery Concept: A Review. *Renew. Sustain. Energy Rev.* **2013**, *21*, 35–51. [[CrossRef](#)]
52. Sobek, S.; Tran, Q.-K.; Junga, R.; Werle, S. Hydrothermal Carbonization of the Waste Straw: A Study of the Biomass Transient Heating Behavior and Solid Products Combustion Kinetics. *Fuel* **2021**, *314*, 122725. [[CrossRef](#)]
53. Czerwińska, K.; Śliz, M.; Wilk, M. Hydrothermal Carbonization Process: Fundamentals, Main Parameter Characteristics and Possible Applications Including an Effective Method of SARS-CoV-2 Mitigation in Sewage Sludge. A Review. *Renew. Sustain. Energy Rev.* **2022**, *154*, 111873. [[CrossRef](#)]
54. Hansen, L.J.; Fendt, S.; Spliethoff, H. Impact of Hydrothermal Carbonization on Combustion Properties of Residual Biomass. *Biomass Convers. Biorefinery* **2022**, *12*, 2541–2552. [[CrossRef](#)]
55. Smith, A.M.; Singh, S.; Ross, A.B. Fate of Inorganic Material during Hydrothermal Carbonisation of Biomass: Influence of Feedstock on Combustion Behaviour of Hydrochar. *Fuel* **2016**, *169*, 135–145. [[CrossRef](#)]
56. Śliz, M.; Tuci, F.; Czerwińska, K.; Fabrizi, S.; Lombardi, L.; Wilk, M. Hydrothermal Carbonization of the Wet Fraction from Mixed Municipal Solid Waste: Hydrochar Characteristics and Energy Balance. *Waste Manag.* **2022**, *151*, 39–48. [[CrossRef](#)] [[PubMed](#)]
57. Śliz, M.; Czerwińska, K.; Magdziarz, A.; Lombardi, L.; Wilk, M. Hydrothermal Carbonization of the Wet Fraction from Mixed Municipal Solid Waste: A Fuel and Structural Analysis of Hydrochars. *Energies* **2022**, *15*, 6708. [[CrossRef](#)]
58. Purnomo, C.; Castello, D.; Fiori, L. Granular Activated Carbon from Grape Seeds Hydrothermal Char. *Appl. Sci.* **2018**, *8*, 331. [[CrossRef](#)]
59. Chung, J.; Edewi, O.; Foppen, J.; Gerner, G.; Krebs, R.; Lens, P. Removal of Escherichia Coli by Intermittent Operation of Saturated Sand Columns Supplemented with Hydrochar Derived from Sewage Sludge. *Appl. Sci.* **2017**, *7*, 839. [[CrossRef](#)]
60. Scrinzi, D.; Andreottola, G.; Fiori, L. Composting Hydrochar-OFMSW Digestate Mixtures: Design of Bioreactors and Preliminary Experimental Results. *Appl. Sci.* **2021**, *11*, 1496. [[CrossRef](#)]
61. Adjuik, T.; Rodjom, A.M.; Miller, K.E.; Reza, M.T.M.; Davis, S.C. Application of Hydrochar, Digestate, and Synthetic Fertilizer to a Miscanthus X Giganteus Crop: Implications for Biomass and Greenhouse Gas Emissions. *Appl. Sci.* **2020**, *10*, 8953. [[CrossRef](#)]
62. Luo, H.; Wang, X.; Liu, X.; Wu, X.; Shi, X.; Xiong, Q. A Review on CFD Simulation of Biomass Pyrolysis in Fluidized Bed Reactors with Emphasis on Particle-Scale Models. *J. Anal. Appl. Pyrolysis* **2022**, *162*, 105433. [[CrossRef](#)]
63. Luo, H.; Liu, X.; Niedzwiecki, L.; Wu, X.; Lin, W.; Lu, B.; Wang, W.; Wu, H. Analysis of Model Dimensionality, Particle Shrinkage, Boundary Layer Reactions on Particle-Scale Modelling of Biomass Char Conversion under Pulverized Fuel Combustion Conditions. *Proc. Combust. Inst.* **2022**. [[CrossRef](#)]

64. Luo, H.; Wang, X.; Krochmalny, K.; Niedzwiecki, L.; Czajka, K.; Pawlak-Kruczek, H.; Wu, X.; Liu, X.; Xiong, Q. Assessments and Analysis of Lumped and Detailed Pyrolysis Kinetics for Biomass Torrefaction with Particle-Scale Modeling. *Biomass Bioenergy* **2022**, *166*, 106619. [[CrossRef](#)]
65. Wang, S.; Persson, H.; Yang, W.; Jönsson, P.G. Pyrolysis Study of Hydrothermal Carbonization-Treated Digested Sewage Sludge Using a Py-GC/MS and a Bench-Scale Pyrolyzer. *Fuel* **2020**, *262*, 116335. [[CrossRef](#)]
66. Liu, Y.; Zhai, Y.; Li, S.; Liu, X.; Wang, B.; Qiu, Z.; Li, C. Production of Bio-Oil with Low Oxygen and Nitrogen Contents by Combined Hydrothermal Pretreatment and Pyrolysis of Sewage Sludge. *Energy* **2020**, *203*, 117829. [[CrossRef](#)]
67. Wang, S.; Wen, Y.; Hammarström, H.; Jönsson, P.G.; Yang, W. Pyrolysis Behaviour, Kinetics and Thermodynamic Data of Hydrothermal Carbonization-Treated Pulp and Paper Mill Sludge. *Renew. Energy* **2021**, *177*, 1282–1292. [[CrossRef](#)]
68. Czajka, K.; Kisiela, A.; Moroń, W.; Ferens, W.; Rybak, W. Pyrolysis of Solid Fuels: Thermochemical Behaviour, Kinetics and Compensation Effect. *Fuel Process. Technol.* **2016**, *142*, 42–53. [[CrossRef](#)]
69. Czajka, K.M. The Impact of the Thermal Lag on the Interpretation of Cellulose Pyrolysis. *Energy* **2021**, *236*, 121497. [[CrossRef](#)]
70. Sobek, S.; Werle, S. Solar Pyrolysis of Waste Biomass: Part 2 Kinetic Modeling and Methodology of the Determination of the Kinetic Parameters for Solar Pyrolysis of Sewage Sludge. *Renew. Energy* **2020**, *153*, 962–974. [[CrossRef](#)]
71. Dudziak, M.; Werle, S.; Marszałek, A.; Sobek, S.; Magdziarz, A. Comparative Assessment of the Biomass Solar Pyrolysis Biochars Combustion Behavior and Zinc Zn(II) Adsorption. *Energy* **2022**, *261*, 125360. [[CrossRef](#)]
72. Louwes, A.C.; Halfwerk, R.B.; Bramer, E.A.; Brem, G. Experimental Study on Fast Pyrolysis of Raw and Torrefied Woody Biomass. *Energy Technol.* **2020**, *8*, 1900799. [[CrossRef](#)]
73. Brem, G.; Bramer, E.A. PyRos: A New Flash Pyrolysis Technology for the Production of Bio-Oil from Biomass Residues. *Bioenergy Outlook* **2007**, 25–27.
74. Meier, D.; Van De Beld, B.; Bridgwater, A.V.; Elliott, D.C.; Oasmaa, A.; Preto, F. State-of-the-Art of Fast Pyrolysis in IEA Bioenergy Member Countries. *Renew. Sustain. Energy Rev.* **2013**, *20*, 619–641. [[CrossRef](#)]
75. Plis, A.; Lasek, J.; Skawińska, A.; Zuwała, J. Thermochemical and Kinetic Analysis of the Pyrolysis Process in Cladophora Glomerata Algae. *J. Anal. Appl. Pyrolysis* **2015**, *115*, 166–174. [[CrossRef](#)]
76. Pawlak-Kruczek, H.; Krochmalny, K.; Mościcki, K.; Zgóra, J.; Czerep, M.; Ostrycharczyk, M.; Niedzwiecki, Ł. Torrefaction of Various Types of Biomass in Laboratory Scale, Batch-Wise Isothermal Rotary Reactor and Pilot Scale, Continuous Multi-Stage Tape Reactor. *Eng. Prot. Environ.* **2017**, *20*, 457–472. [[CrossRef](#)]
77. Pawlak-Kruczek, H.; Krochmalny, K.; Wnukowski, M.; Niedzwiecki, L. Slow Pyrolysis of the Sewage Sludge with Additives: Calcium Oxide and Lignite. *J. Energy Resour. Technol.* **2018**, *140*, 062206. [[CrossRef](#)]
78. Mościcki, K.J.; Niedzwiecki, L.; Owczarek, P.; Wnukowski, M. Commoditization of Biomass: Dry Torrefaction and Pelletization—A Review. *J. Power Technol.* **2014**, *94*, 233–249.
79. Poudel, J.; Karki, S.; Gu, J.H.; Lim, Y.; Oh, S.C. Effect of Co-Torrefaction on the Properties of Sewage Sludge and Waste Wood to Enhance Solid Fuel Qualities. *J. Residuals Sci. Technol.* **2017**, *14*, 23–36. [[CrossRef](#)]
80. Pułka, J.; Wiśniewski, D.; Gołaszewski, J.; Białowiec, A. Is the Biochar Produced from Sewage Sludge a Good Quality Solid Fuel? *Arch. Environ. Prot.* **2016**, *42*, 125–134. [[CrossRef](#)]
81. Mihajlović, M.; Petrović, J.; Maletić, S.; Isakovski, M.K.; Stojanović, M.; Lopičić, Z.; Trifunović, S. Hydrothermal Carbonization of *Miscanthus × giganteus*: Structural and Fuel Properties of Hydrochars and Organic Profile with the Ecotoxicological Assessment of the Liquid Phase. *Energy Convers. Manag.* **2018**, *159*, 254–263. [[CrossRef](#)]
82. Wilk, M.; Magdziarz, A. Hydrothermal Carbonization, Torrefaction and Slow Pyrolysis of *Miscanthus Giganteus*. *Energy* **2017**, *140*, 1292–1304. [[CrossRef](#)]
83. Kambo, H.S.; Dutta, A. Comparative Evaluation of Torrefaction and Hydrothermal Carbonization of Lignocellulosic Biomass for the Production of Solid Biofuel. *Energy Convers. Manag.* **2015**, *105*, 746–755. [[CrossRef](#)]
84. Reza, M.T.; Lynam, J.G.; Uddin, M.H.; Coronella, C.J. Hydrothermal Carbonization: Fate of Inorganics. *Biomass Bioenergy* **2013**, *49*, 86–94. [[CrossRef](#)]
85. Aragón-Briceño, C.I.; Ross, A.B.; Camargo-Valero, M.A. Mass and Energy Integration Study of Hydrothermal Carbonization with Anaerobic Digestion of Sewage Sludge. *Renew. Energy* **2021**, *167*, 473–483. [[CrossRef](#)]
86. Aragón-Briceño, C.I.; Grasham, O.; Ross, A.B.; Dupont, V.; Camargo-Valero, M.A. Hydrothermal Carbonization of Sewage Digestate at Wastewater Treatment Works: Influence of Solid Loading on Characteristics of Hydrochar, Process Water and Plant Energetics. *Renew. Energy* **2020**, *157*, 959–973. [[CrossRef](#)]
87. Wilk, M.; Magdziarz, A.; Kalembe-Rec, I.; Szymańska-Chargot, M. Upgrading of Green Waste into Carbon-Rich Solid Biofuel by Hydrothermal Carbonization: The Effect of Process Parameters on Hydrochar Derived from Acacia. *Energy* **2020**, *202*, 117717. [[CrossRef](#)]
88. Wilk, M.; Magdziarz, A.; Jayaraman, K.; Szymańska-Chargot, M.; Gökalp, I. Hydrothermal Carbonization Characteristics of Sewage Sludge and Lignocellulosic Biomass. A Comparative Study. *Biomass Bioenergy* **2019**, *120*, 166–175. [[CrossRef](#)]
89. Kumar, N.; Weldon, R.; Lynam, J.G. Hydrothermal Carbonization of Coffee Silverskins. *Biocatal. Agric. Biotechnol.* **2021**, *36*, 102145. [[CrossRef](#)]
90. Lucantonio, S.; Di Giuliano, A.; Gallucci, K. Influences of the Pretreatments of Residual Biomass on Gasification Processes: Experimental Devolatilizations Study in a Fluidized Bed. *Appl. Sci.* **2021**, *11*, 5722. [[CrossRef](#)]

91. Hansen, L.J.; Fendt, S.; Spliethoff, H. Comparison of Fuels and Effluents Originating from Washing and Hydrothermal Carbonisation of Residual Biomass. *Waste Biomass Valorization* **2022**, *13*, 2321–2333. [\[CrossRef\]](#)
92. Gao, L.; Volpe, M.; Lucian, M.; Fiori, L.; Goldfarb, J.L. Does Hydrothermal Carbonization as a Biomass Pretreatment Reduce Fuel Segregation of Coal-Biomass Blends during Oxidation? *Energy Convers. Manag.* **2019**, *181*, 93–104. [\[CrossRef\]](#)
93. Ferrentino, R.; Ceccato, R.; Marchetti, V.; Andreottola, G.; Fiori, L. Sewage Sludge Hydrochar: An Option for Removal of Methylene Blue from Wastewater. *Appl. Sci.* **2020**, *10*, 3445. [\[CrossRef\]](#)
94. Gallucci, K.; Taglieri, L.; Papa, A.A.; Di Lauro, F.; Ahmad, Z.; Gallifuoco, A. Non-Energy Valorization of Residual Biomasses via HTC: CO₂ Capture onto Activated Hydrochars. *Appl. Sci.* **2020**, *10*, 1879. [\[CrossRef\]](#)
95. Channiwala, S.A.; Parikh, P.P. A Unified Correlation for Estimating HHV of Solid, Liquid and Gaseous Fuels. *Fuel* **2002**, *81*, 1051–1063. [\[CrossRef\]](#)
96. Friedl, A.; Padouvas, E.; Rotter, H.; Varmuza, K. Prediction of Heating Values of Biomass Fuel from Elemental Composition. *Anal. Chim. Acta* **2005**, *544*, 191–198. [\[CrossRef\]](#)
97. Sallevelt, J.L.H.P.; Gudde, J.E.P.; Pozarlik, A.K.; Brem, G. The Impact of Spray Quality on the Combustion of a Viscous Biofuel in a Micro Gas Turbine. *Appl. Energy* **2014**, *132*, 575–585. [\[CrossRef\]](#)
98. Sallevelt, J.L.H.P.; Pozarlik, A.K.; Brem, G. Characterization of Viscous Biofuel Sprays Using Digital Imaging in the Near Field Region. *Appl. Energy* **2015**, *147*, 161–175. [\[CrossRef\]](#)
99. Bhakta Sharma, H.; Panigrahi, S.; Dubey, B.K. Food Waste Hydrothermal Carbonization: Study on the Effects of Reaction Severities, Pelletization and Framework Development Using Approaches of the Circular Economy. *Bioresour. Technol.* **2021**, *333*, 125187. [\[CrossRef\]](#)
100. Romanowska-Duda, Z.; Szufa, S.; Grzesik, M.; Piotrowski, K.; Janas, R. The Promotive Effect of Cyanobacteria and *Chlorella* sp. Foliar Biofertilization on Growth and Metabolic Activities of Willow (*Salix viminalis* L.) Plants as Feedstock Production, Solid Biofuel and Biochar as C Carrier for Fertilizers via Torrefaction Proce. *Energies* **2021**, *14*, 5262. [\[CrossRef\]](#)
101. Szufa, S.; Piersa, P.; Adrian, Ł.; Czerwińska, J.; Lewandowski, A.; Lewandowska, W.; Sielski, J.; Dzikuc, M.; Wróbel, M.; Jewiarz, M.; et al. Sustainable Drying and Torrefaction Processes of Miscanthus for Use as a Pelletized Solid Biofuel and Biocarbon-Carrier for Fertilizers. *Molecules* **2021**, *26*, 1014. [\[CrossRef\]](#)
102. Szufa, S.; Piersa, P.; Adrian, Ł.; Sielski, J.; Grzesik, M.; Romanowska-Duda, Z.; Piotrowski, K.; Lewandowska, W. Acquisition of Torrefied Biomass from Jerusalem Artichoke Grown in a Closed Circular System Using Biogas Plant Waste. *Molecules* **2020**, *25*, 3862. [\[CrossRef\]](#)
103. Brachi, P.; Miccio, F.; Miccio, M.; Ruoppolo, G. Torrefaction of Tomato Peel Residues in a Fluidized Bed of Inert Particles and a Fixed-Bed Reactor. *Energy Fuels* **2016**, *30*, 4858–4868. [\[CrossRef\]](#)
104. Gucho, E.; Shahzad, K.; Bramer, E.; Akhtar, N.; Brem, G. Experimental Study on Dry Torrefaction of Beech Wood and Miscanthus. *Energies* **2015**, *8*, 3903–3923. [\[CrossRef\]](#)
105. Ribeiro, J.M.C.; Godina, R.; Matias, J.C.d.O.; Nunes, L.J.R. Future Perspectives of Biomass Torrefaction: Review of the Current State-of-the-Art and Research Development. *Sustainability* **2018**, *10*, 2323. [\[CrossRef\]](#)
106. Szwaja, S.; Magdziarz, A.; Zajemska, M.; Poskart, A. A Torrefaction of Sida Hermaphrodita to Improve Fuel Properties. Advanced Analysis of Torrefied Products. *Renew. Energy* **2019**, *141*, 894–902. [\[CrossRef\]](#)
107. Jaworski, T.J.; Kajda-Szcześniak, M. Study on the Similarity of the Parameters of Biomass and Solid Waste Fuel Combustion for the Needs of Thermal Power Engineering. *Sustainability* **2020**, *12*, 7894. [\[CrossRef\]](#)
108. Botelho, T.; Costa, M.; Wilk, M.; Magdziarz, A. Evaluation of the Combustion Characteristics of Raw and Torrefied Grape Pomace in a Thermogravimetric Analyzer and in a Drop Tube Furnace. *Fuel* **2018**, *212*, 95–100. [\[CrossRef\]](#)
109. Mlonka-Mędrala, A.; Magdziarz, A.; Dziok, T.; Sieradzka, M.; Nowak, W. Laboratory Studies on the Influence of Biomass Particle Size on Pyrolysis and Combustion Using TG GC/MS. *Fuel* **2019**, *252*, 635–645. [\[CrossRef\]](#)
110. Kumar, A.; Monika; Mishra, R.K.; Jaglan, S. Pyrolysis of Low-Value Waste Miscanthus Grass: Physicochemical Characterization, Pyrolysis Kinetics, and Characterization of Pyrolytic End Products. *Process Saf. Environ. Prot.* **2022**, *163*, 68–81. [\[CrossRef\]](#)
111. Matusiak, M.; Słezak, R.; Ledakowicz, S. Thermogravimetric Kinetics of Selected Energy Crops Pyrolysis. *Energies* **2020**, *13*, 3977. [\[CrossRef\]](#)
112. Cortés, A.M.; Bridgwater, A.V. Kinetic Study of the Pyrolysis of Miscanthus and Its Acid Hydrolysis Residue by Thermogravimetric Analysis. *Fuel Process. Technol.* **2015**, *138*, 184–193. [\[CrossRef\]](#)
113. Asadullah, M. Biomass Gasification Gas Cleaning for Downstream Applications: A Comparative Critical Review. *Renew. Sustain. Energy Rev.* **2014**, *40*, 118–132. [\[CrossRef\]](#)

Disclaimer/Publisher’s Note: The statements, opinions and data contained in all publications are solely those of the individual author(s) and contributor(s) and not of MDPI and/or the editor(s). MDPI and/or the editor(s) disclaim responsibility for any injury to people or property resulting from any ideas, methods, instructions or products referred to in the content.